SAND78-0381

Unlimited Release
UC-62

Performance Testing of the Hexcel Parabolic Trough Solar Collector

Vernon E. Dudley, EG&G, Inc.
Robert M. Workhoven

Prepared by Sandia Laboratories, Albuquerque, New Mexico 87115 and Livermore, California 94550 for the United States Department of Energy under Contract AT(29-1)-789

Printed March 1978

Sandia Laboratories

Printed in the United States of America

Available from
National Technical Information Service
U. S. Department of Commerce
5285 Port Royal Road
Springfield, VA 22161

Price: Printed Copy **$3.50** ; Microfiche $3.00

Issued by Sandia Laboratories, operated for the United States
Department of Energy by Sandia Corporation

SAND78-0381
Unlimited Release
Printed March 1978

PERFORMANCE TESTING OF THE HEXCEL PARABOLIC TROUGH SOLAR COLLECTOR

Vernon E. Dudley
EG&G, Inc.

Robert M. Workhoven
Solar Total Energy Test Facility Division 5712
Sandia Laboratories
Albuquerque, NM 87115

ABSTRACT

This report summarizes the testing which was performed on the Hexcel Parabolic Trough Solar Collector at the Solar Total Energy Test Facility. Test objectives are defined, test procedures are described, and results and conclusions are given.

CONTENTS

ILLUSTRATIONS

TABLES

PERFORMANCE TESTING OF THE
HEXCEL PARABOLIC TROUGH SOLAR COLLECTOR

INTRODUCTION: A series of solar collector designs are being tested in the Sandia Laboratories Collector Module Test Facility as a part of the Department of Energy's continuing program to characterize selected collector modules for possible future system use (Reference 1). Several of the collector designs tested have been chosen to provide the energy input for large demonstration projects throughout the nation. The Hexcel Solar Collector evaluated for this report is commercially available. A series of similar collectors is currently providing power for a 50 hp irrigation pump motor at Casa Grande, AZ. The design has also been selected for a 2800 m^2 (30,000 ft^2) collector field at the Indian Health Center project at White River, AZ and a 1580 m^2 (17,000 ft^2) collector field at Yuma, AZ.

TEST OBJECTIVE: The objective of this test series was to characterize the performance of a parabolic trough concentrating solar collector module manufactured by the Hexcel Corporation of Dublin, CA. Items of particular interest were the peak thermal efficiency at solar noon and the receiver tube thermal losses at fluid temperatures from 150°C to 300°C.

COLLECTOR DESCRIPTION: The Hexcel concentrator system (Figure 1) consisted of four mirror panels arranged to form a linear focus parabolic reflector. Focal

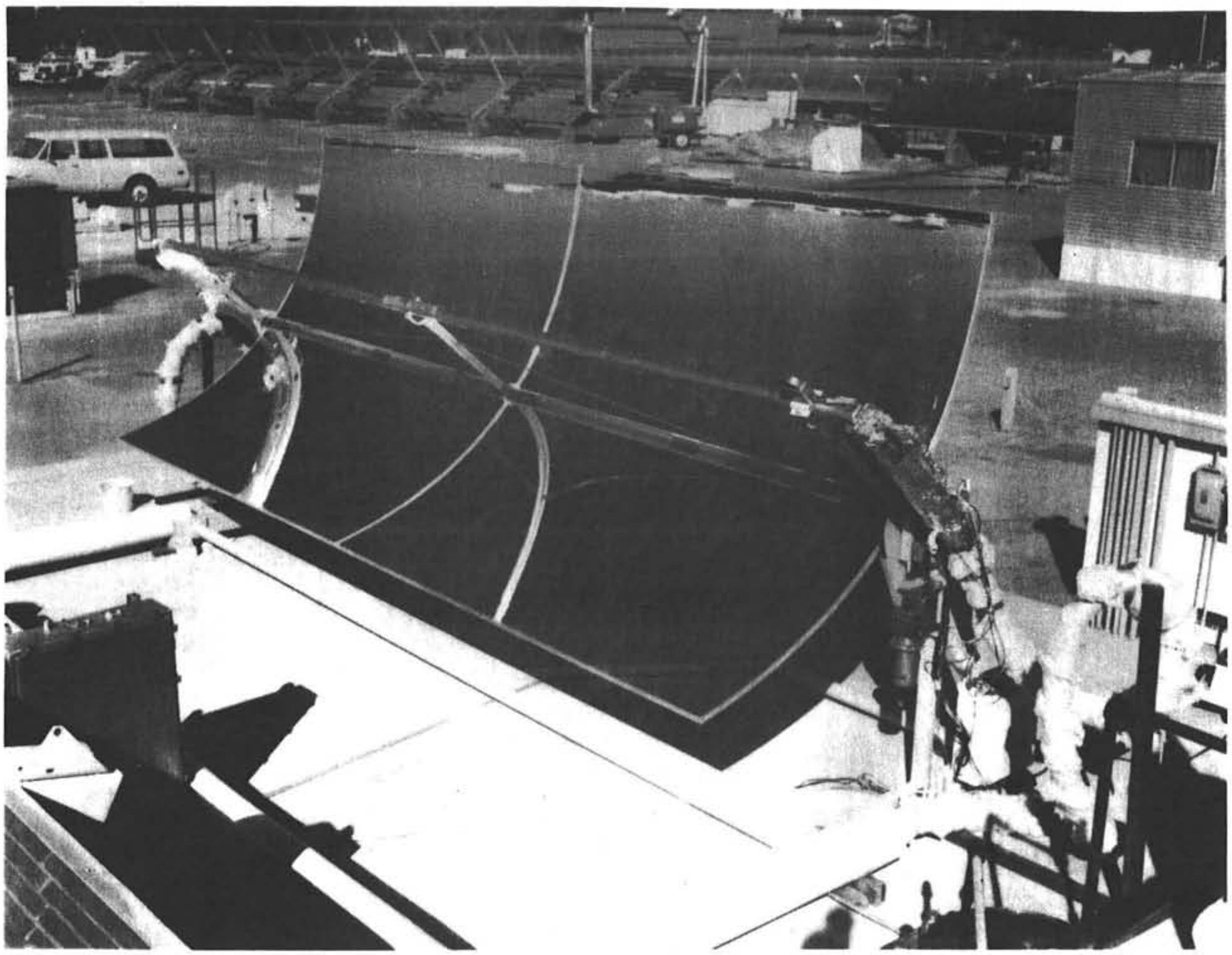

Figure 1. Hexcel Collector

length was 0.914 m (36 in.); rim angle was 72°. The mirror panels were 3/8 inch aluminum honeycomb sandwich construction with 1/2 inch aluminum channel protecting the edges. The reflecting surface was FEK 163, an aluminized second-surface acrylic film manufactured by 3M Corporation. Each mirror panel was 2.98 m in length and 1.41 m in width and weighed about 16 kg.

In most parabolic trough concentrator designs, the mirror is a one piece assembly. In such a design, the receiver tube assembly casts a shadow along the center line of the mirror. The shadowed area is not effective in concentrating energy upon the absorber tube but is included in the mirror aperture area.

In the Hexcel design, advantage was taken of the centerline shadow to make the mirror in halves. The resulting centerline gap of approximately 7.5 cm between mirror halves was fully shadowed by the receiver assembly; this shadowed area was included in the mirror aperture area for consistency with the other designs tested. Thus, the mirror aperture used for efficiency calculations was 15.91 m^2, actual reflective surface aperture area was 15.49 m^2.

The steel absorber tube was 6.4 m in length, (approximately 30 cm longer than the mirror) with 3.81 cm outside diameter and 3.18 cm inside diameter. The absorber tube had spiral internal grooves resembling the rifling in a gun barrel (Figure 2), with a 3.02 cm internal plug tube to confine the fluid flow to the tube wall area. The outer surface of the absorber was plated with a selective black chrome to enhance solar radiation absorption and reduce radiated thermal loss. To further reduce losses from the absorber tube, a half-cylinder of pyrex glass was fitted over the tube on the radiation absorbing side. The back half of

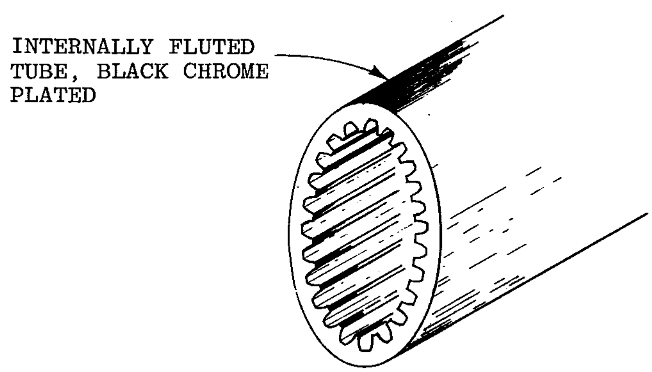

Figure 2. Absorber Tube Construction.

the tube was covered with a double layer metal shield (Figure 3); insulation was placed between the two layers to reduce losses. The inner layer was polished aluminum to reflect radiation back onto the absorber tube.

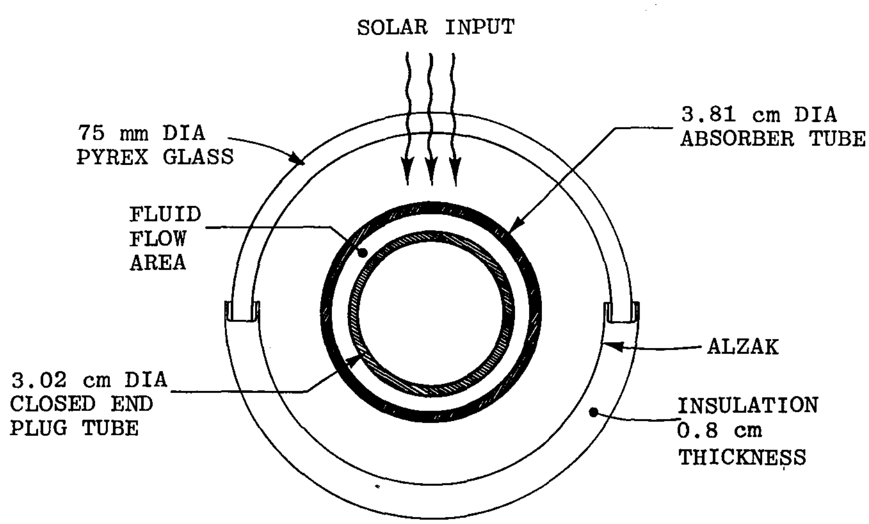

Figure 3. Receiver Assembly.

The collector supporting structure was constructed from welded steel tubing. Total weight of the complete module as tested at Sandia was about 580 kg. As configured for a large collector field, weight would be about 435 kg. A Delavan Electronics Corporation Sun-Trak sun sensor and the tracking system electronics were mounted at one end of the collector module, with a 24 volt dc motor providing power to move the mirror system for sun tracking. The collector system was oriented E-W, tracking the sun in elevation only.

TEST FACILITY DESCRIPTION: General features of the Therminol fluid loop system used for this test can be found in Reference 2. Installation of the Hexcel Collector module began on 4 October 1977. Various problems with pipe fittings and insulation delayed completion of installation until 14 October; data collection began on 15 October. A series of excellent sunny days enabled completion of measurements by 25 October. Mr. D. Parker, Hexcel Project Engineer, provided able assistance throughout the test period, and has completed preliminary analysis of the test results (Reference 3).

Each day's testing began by heating the fluid loop with electric heaters to the desired collector input temperature. Usually only one temperature point was attempted in one day due to the time required for temperature stabilization and the need to conduct efficiency tests near solar noon to minimize end effects. The collector system was placed in focus as early as feasible each day so that recovered solar heat could aid in reaching the desired temperature. Temperatures below about 200°C could be attained by about 10:00 am without difficulty; higher temperatures required more time due to increasing losses. Temperatures over 250°C could not be reached before noon without help from the collector system. For each test, input temperature and flow-rate were maintained constant; output temperature varied according to test conditions.

The flow-rate of the Therminol 66 working fluid through the system was measured with a PRI-102A turbine flowmeter manufactured by Flow Technology, Inc. Flow was also measured with a Ramapo SGA-101RM strain gage flowmeter. The flowmeter calibration was checked prior to the test by flowing fluid into a tank and plotting tank weight vs. time. A set of 3 calibrated iron-constantan thermocouples was installed at each end of the collector to determine temperatures into and out of the absorber tube. One thermocouple from each end of the absorber tube was connected as a differential pair for determining the delta temperature for calculations of heat gain or loss (see Figure 4 for thermocouple locations). A Kinics Corporation static mixer was installed at each end of the absorber tube to insure thorough fluid mixing prior to measuring fluid temperature. Direct solar insolation was measured with an Eppley NIP pyrheliometer. Differential pressure from end to end of the absorber tube was measured with a Rosemont pressure transducer. Four absorber tube skin temperatures were measured with iron-constantan thermocouples welded to the outer tube surface (see Figure 4). Ambient temperature, wind direction and wind speed measurements completed the active data collection.

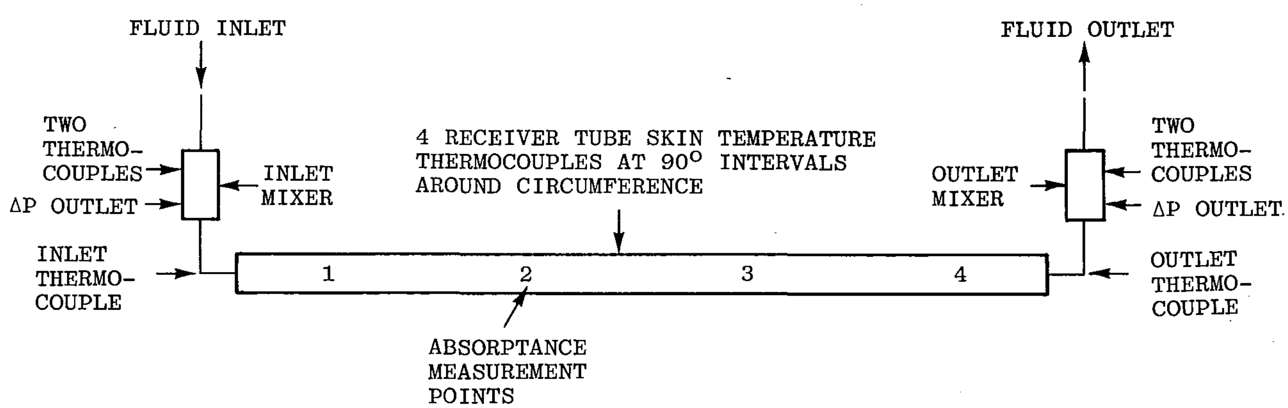

Figure 4. Measurements on Receiver Tube.

The data from the instruments described above were converted to digital format by Doric 210 and 220 analog-to-digital data systems. An HP 2116 minicomputer processed the data and a printout was made of critical data while the test was underway.

Figure 5 is a typical printout of data obtained during an efficiency test. Figure 6 is a sample of data from a thermal loss test. In both figures, temperatures shown are in degrees Fahrenheit. Delta temperature shown is not the difference between the input and output temperatures printed; this value was obtained from the pair of differential thermocouples mentioned above. Speed of the data system was such that all the data channels could be read, calculations performed, and a line in the data table printed in about 15 seconds. The average values were automatically printed after ten data points were accumulated. The complete data printout as shown in Figures 5 and 6 ran continuously, repeating at intervals of about three minutes throughout a test run. Forty measured and calculated data values, plus ten average values were available from the data system every 15 seconds. Only the data shown in Figures 5 and 6 were printed; the remaining data would normally be recorded on magnetic tape for later analysis. The number of decimal places printed in Figures 5 and 6 should not be taken as indicating the data system accuracy; choice of the print format was dictated by pecularities of the computer system used. Only those data blocks occurring under stable conditions are included in this report.

HEXCEL COLLECTOR EFFICIENCY TEST

JULIAN DAY 292 HOUR 12 MINUTE 1 SOLAR TIME

69.2 AMBIENT TEMPERATURE (DEG F)
267 WIND DIRECTION, DEGREES
3 WIND SPEED, MPH

SKIN TEMPS-0,90, 180, 270 DEG 464.2 453.4 462.6
462.1

TEMP IN	TEMP OUT	SOLAR BTU/HR FT 2	DELTA TEMP	FLOW GPM	EFFICIENCY PERCENT
446.8	473.7	322.23	25.7	5.27	57.2
446.8	473.7	322.52	25.7	5.26	57.2
446.9	473.7	322.64	25.7	5.27	57.3
446.9	473.7	322.56	25.6	5.27	57
447	473.7	322.85	25.6	5.27	56.9
447	473.8	322.85	25.7	5.27	57.2
447	473.9	322.89	25.7	5.26	57.1
446.9	473.8	322.47	25.8	5.26	57.4
447	473.8	322.56	25.7	5.26	57.2
446.9	473.8	322.35	25.8	5.26	57.4
		10 POINT AVERAGES			
446.92	473.76	322.592	25.7	5.265	57.19

7.15525E-06 AVERAGE KINEMATIC VISCOSITY
6.94739 AVERAGE DENSITY
2.33050E-02 AVERAGE FRICTION FACTOR
10.395 AVERAGE DIFFERENTIAL PRESSURE

DIFFERENTIAL THERMOCOUPLES USED FOR DELTA T AND EFFICIENCY

END OF DATA PASS 4

Figure 5. Efficiency Test Data Printout

HEXCEL THERMAL LOSS TEST

JULIAN DAY 295 HOUR 13 MINUTE 4 SOLAR TIME

65.8	AMBIENT TEMPERATURE (DEG F)
112	WIND DIRECTION, DEGREES
7	WIND SPEED, MPH

SKIN TEMPS-0,90, 180, 270 DEG 514.7 569.9 518 518.3

TEMP IN	TEMP OUT	FLOW GPM	DELTA TEMP	BTU/HR GAIN
519.7	516.1	5.38	-4.4	-5132.02
519.7	516.1	5.38	-4.3	-5012.45
519.6	516.1	5.37	-4.4	-5119.23
519.6	516.1	5.37	-4.3	-5006.16
519.6	516.1	5.36	-4.4	-5114.31
519.7	516.2	5.37	-4.4	-5125.83
519.6	516.2	5.37	-4.3	-5009.2
519.6	516.1	5.36	-4.2	-4889.09
519.6	516.1	5.36	-4.3	-5000.68
519.6	516.1	5.38	-4.4	-5130.02
	10 POINT AVERAGES			
519.63	516.12	5.37	-4.34	-5053.09

-14.69	EFFICIENCY IN PERCENT. (INCORRECT EXCEPT AT SOLAR NOON)
202.794	AVERAGE SOLAR INSOLATION, BTU/HR SQ FT
9.95	AVERAGE DIFFERENTIAL PRESSURE
1.96834E-02	AVERAGE FRICTION FACTOR
2950.44	AVERAGE REYNOLDS NUMBER

END OF DATA PASS 11

Figure 6. Thermal Loss Data Printout

PERFORMANCE TEST DEFINITIONS: During a test run, specific heat and density of the Therminol 66 fluid were calculated for each data set using the average temperature of the fluid in the absorber tube and fluid properties furnished by Monsanto Industrial Chemicals Company (Reference 4). Heat gain (or loss) was then calculated from

$$Q = \dot{m}\, C_p\, \Delta T$$

where

Q = heat gain, kJ/hr

$\dot{m}$ = mass flow rate of fluid, kg/hr

C_p = specific heat of fluid, J/kg^{O}C

ΔT = in-out temperature differential, ^{O}C

A successful loss measurement was one in which the values for input and output temperatures remained constant to within 0.1^{O}C or less, flow-rate varied by 0.1 liter/min or less and delta temperature changed by 0.1^{O}C or less. Most loss test data points reported are averages of four-to-six ten point data blocks, each block judged stable as described above, and with conditions nearly constant over the entire time averaged. Loss tests were conducted with the collector system near its normal operating position, but defocused sufficiently so that no light from the mirror would strike any part of the receiver assembly.

On most days, after reaching the desired temperature, loss measurements were made until about one hour before noon. Loss testing was resumed for about two hours after completion of solar noon efficiency tests; the fluid loop was then placed in a cooling mode prior to shutdown for the day.

For an efficiency test, efficiency was calculated from

$$\eta = \frac{Q/A}{I}$$

where

η = solar collector efficiency
Q = heat gain, W
A = collector aperture area, m^2
I = solar insolation, W/m^2

An efficiency measurement at a single temperature and flow-rate was usually made from about one hour before noon until about one hour after noon to insure complete temperature and flow stabilization. This procedure insured good definition of the peak noon efficiency. The all day efficiency tests were run at a constant flow-rate and input temperature without interruption for the entire day to define the concentrator's efficiency at various sun angles. These tests began as early as operating temperatures could be established and continued until efficiency reached zero (zero net heat gain).

A "good" efficiency data point consists of at least one of the ten point averages during which input and output temperatures changed by 0.1°C or less, flow-rates varied by 0.1 liter/minute or less, delta temperature remained within 0.1°C or less, and solar insolation remained constant to about 1%. Temperatures, flow-rate and insolation had to have been nearly as stable as described above for at least five to ten minutes prior to the "good" data point to be believable. Except for the continuous all-day test runs, efficiency measurements were not normally made except near solar noon, and with an insolation greater than about 950 watts/m^2.

Prior to beginning thermal testing of the Hexcel collector, measurements were made to determine the solar spectrum absorptance and emittance of the absorber tube's black chrome coating. These measurements were made with a Gier-Dunkle Infrared Reflectometer, Model DB-100, at intervals each side of center on the absorber tube. Measurement positions are indicated in Figure 4. The measurements were repeated after conclusion of the thermal testing.

Differential pressure from end-to-end of the absorber tube was measured throughout the test series for all the temperatures and flow-rates used. These values were not printed continuously, but ten point averages were printed at the end of each three minute data block. Differential pressure indicates the pumping power that may be required at various temperatures and flow-rates and was also used in calculating friction factor and Reynolds numbers for the system.

TEST RESULTS: Table 1 shows tabulated values obtained near solar noon during the efficiency tests. These values are plotted in Figure 7 to obtain a curve of peak noon efficiency vs. fluid output temperature. Flow-rates were varied from 11 to 28 liters/min (approximately 3 to 7 gallons/min). Measured peak efficiencies ranged from 64% at 160°C to 56% at 300°C.

Table 1. Hexcel Collector Peak Noon Efficiency

Test Date	Temperature Out (°C)	Receiver Tube (ΔT°C)	Flow-Rate (liters/min)	Efficiency (%)	Solar Insolation (W/m²)
10/15/77	167.2	9.4	31.4	62	946
10/17/77	168.8	16.3	19.9	64	1006
10/18/77	161.6	11.7	28.4	64	1021
10/19/77	245.4	14.3	19.9	57	1015
10/20/77	241.3	10.3	27.4	59	987
10/21/77	226.7	20.8	13.6	58	1006
10/23/77	299.2	9.4	26.6	56	946
10/24/77	304.0	13.6	19.3	55	999
10/25/77	312.2	23.4	11.5	56	1009

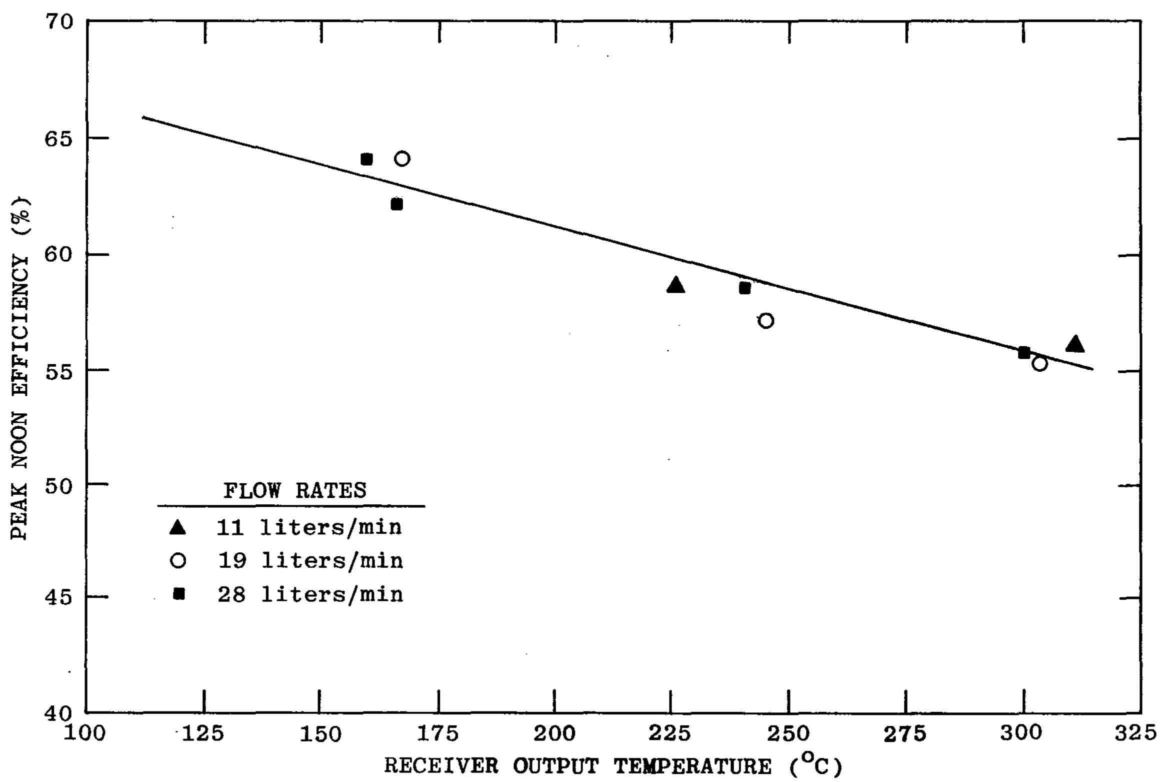

Figure 7. Efficiency of Hexcel Collector.

Figure 8 illustrates the measured collector performance throughout the day when operated at a constant input temperature and constant flow-rate. The solar insolation curve is that measured on 17 October and 25 October during these two efficiency tests; insolation was nearly identical on both days. The efficiency curves begin late in the morning due to the time required to heat and stabilize the fluid loop system at the desired input temperature

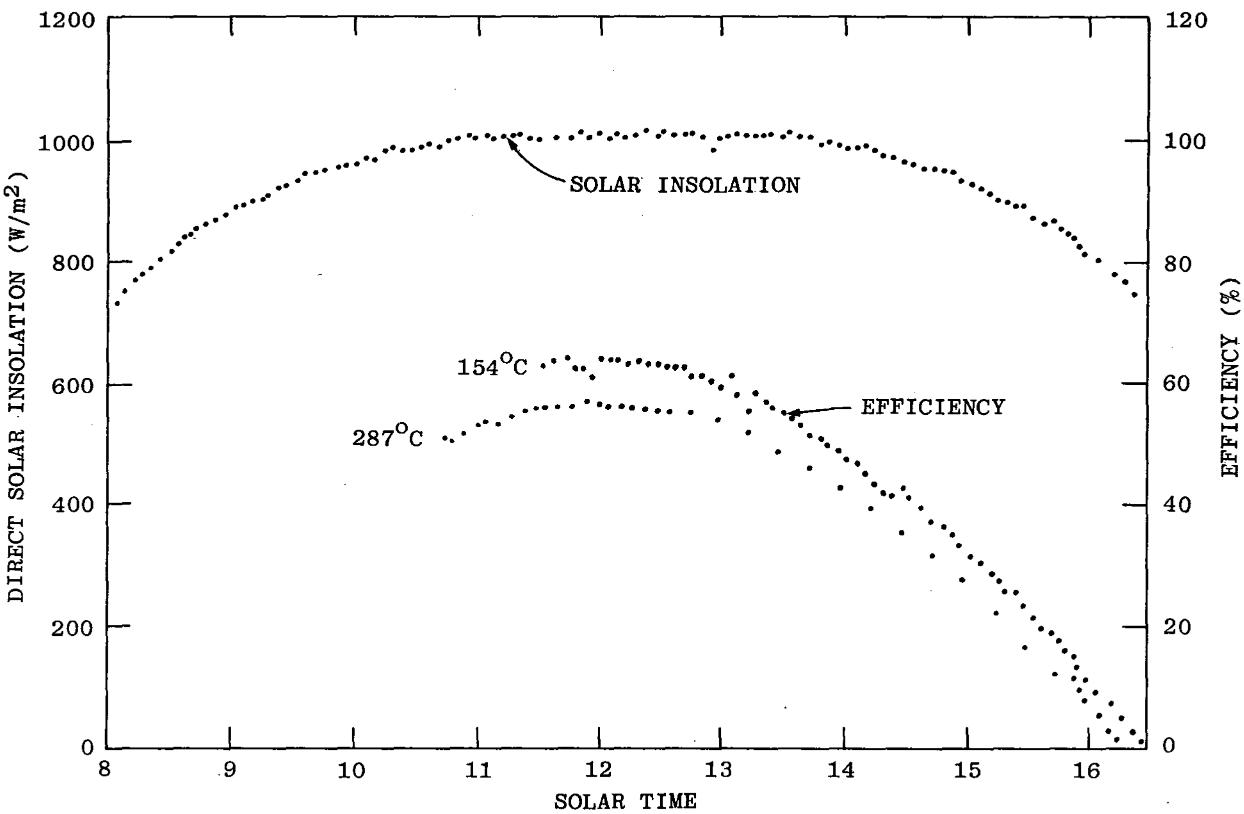

Figure 8. Hexcel All Day Efficiency.

The top efficiency curve in Figure 8 was obtained 17 October 1977 with an input temperature of 154°C and a flow-rate of 19 liters/min. Maximum output temperature was 171°C shortly after noon. Total energy delivered from 1130 to 1630 hours was about 7.3 MJ/m^2. Other collectors have shown symmetrical performance, morning and afternoon. Assuming the early morning portion of this curve would be symmetrical with the afternoon portion, about 12.2 MJ/m^2 could be obtained from a single Hexcel collector module in an 8 hour period. It should be noted that the Hexcel absorber tube extended 30 cm beyond the east end of the mirror. The impact of this asymmetry on the reported data is estimated to be small.

The lower efficiency curve resulted from an input temperature of 287°C and a flow-rate of 11.5 liters/min on 25 October 1977. Maximum output temperature of 312°C occurred at noon. Total energy delivered over the time period shown was about 7.7 MJ/m^2. Again assuming symmetry, about 10.9 MJ/m^2 would be delivered from this module during an 8 hour period. Less end loss would occur when similar modules are placed in long East-West rows in a typical collector field, so the energy delivered per module would be larger.

Another long period efficiency run was attempted on 21 October at an input temperature of 225°C; intermittent clouds prevented obtaining smooth data. Several selected points from this test were checked against Figure 8. As expected, they fell between the two efficiency curves shown.

Some difficulty with the tracking system was encountered during the long efficiency runs. Over a period of about an hour, the tracking would degrade enough to reduce efficiency about 2%; these are the steps visible on the 154°C curve in Figure 8. After readjusting tracking for optimum focus, the problem would appear an hour or so later. This difficulty was apparently not due to a malfunction of the tracking equipment, but probably was due to a misalignment of the tracking photosensors with the collectors.

Table 2 contains the data accumulated during the receiver thermal loss testing. Thermal loss vs. fluid inlet temperature is shown in Figure 9.

Table 2. Hexcel Losses

Test Date	Input Temp (°C)	Receiver ΔT (°C)	Flow (liters/min)	Loss (kJ/hr)	Wind (m/sec)	Ambient Temp (°C)	Solar Insolation* (W/m²)
10/15/77	148.9	0.9	19.6	2026	6.7	16.1	946
10/15/77	147.8	1.7	11.9	2179	6.7	16.7	946
10/15/77	142.2	4.2	4.6	2098	6.7	17.2	955
10/15/77	150.0	0.5	31.2	1567	4.5	18.3	949
10/15/77	216.1	0.8	29.5	2787	1.3	19.4	939
10/15/77	214.4	1.5	19.0	2767	2.7	20.6	946
10/15/77	211.7	2.7	11.4	2971	2.7	20.0	939
10/15/77	203.6	7.0	3.6	3199	2.2	20.6	939
10/18/77	152.4	0.6	27.3	1741	2.2	24.4	984
10/18/77	151.9	0.9	18.8	1885	1.8	24.4	962
10/19/77	229.3	1.2	28.1	3756	1.3	23.3	980
10/19/77	228.0	1.6	21.3	3983	1.3	23.9	968
10/19/77	225.7	3.3	10.8	4072	3.1	24.4	943
10/20/77	227.8	1.6	26.4	4385	3.1	22.8	977
10/22/77	273.7	1.8	29.1	5152	4.5	18.9	892
10/22/77	271.7	2.4	20.3	5337	4.5	18.3	735
10/23/77	283.3	2.8	17.2	5690	1.3	18.3	946
10/23/77	287.8	1.8	26.9	5671	0.5	18.3	946
10/24/77	277.8	4.1	11.4	5526	1.3	21.1	939
10/24/77	283.1	2.4	19.2	5461	1.3	20.0	974

*Direct solar insolation incident on receiver tube assembly during loss test

Thermal loss data has been shown in many ways in previous solar test reports. To facilitate comparisons with other reports, the loss data from the Hexcel test has been plotted in several different formats.

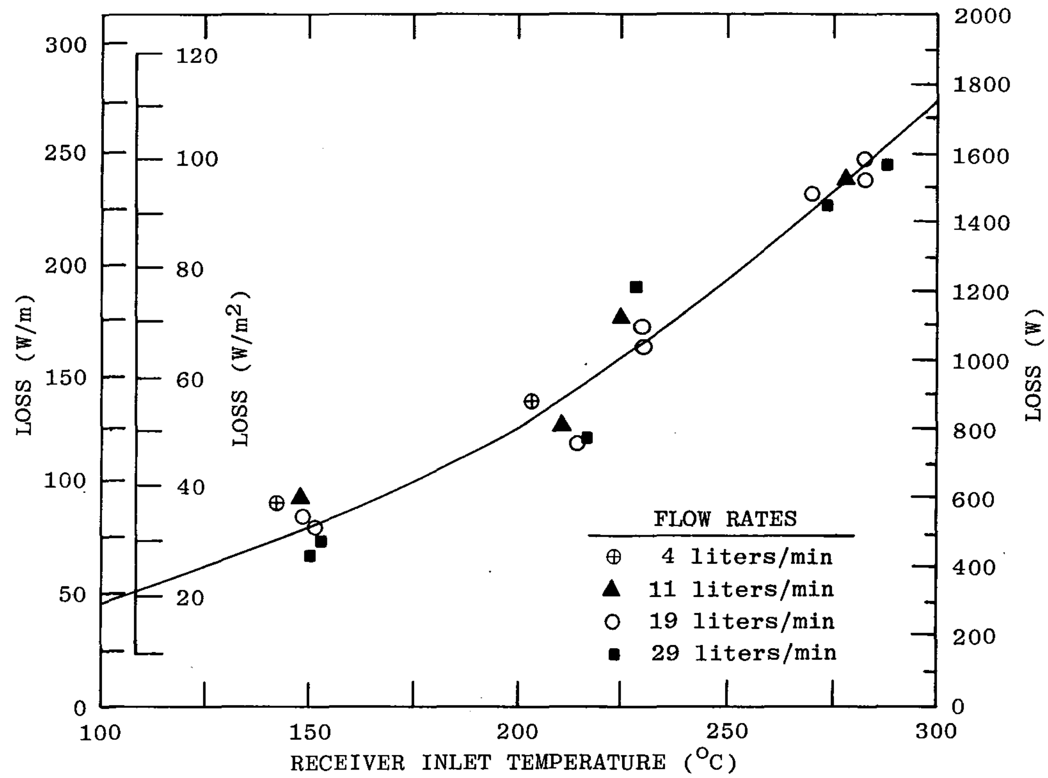

Figure 9. Hexcel Receiver Thermal Loss.

The right ordinate in Figure 9 shows measured thermal loss from the receiver assembly. The left ordinates show thermal loss per unit length of the absorber tube and thermal loss per unit area of the collector aperture. The loss curve was extended to lower temperatures than actually tested by assuming zero losses at approximately 20°C ambient temperatures.

Measured values of differential pressure across the absorber tube are shown in Table 3 for several flow rates and fluid temperatures. Calculated Reynolds numbers are also given in Table 3. Figure 10 shows absorber tube differential pressures vs. flow rates.

Table 3. Absorber Tube Differential Pressures.

Average Temperature (°C)	Flow (liters/min)	Reynolds Number	ΔP (kPa)
154	13.9	--	55.4
152	18.8	2950	87.9
153	27.3	4339	157.3
156	31.3	--	196.7
216	29.4	9388	145.6
214	18.9	5993	69.4

Table 3. Absorber Tube Differential Pressures (Cont)

Average Temperature (°C)	Flow (liters/min)	Reynolds Number	ΔP (kPa)
211	11.3	3462	20.7
202	3.6	1014	9.76
288	26.6	15048	106.5
282	17.2	9415	50.8
276	11.4	5980	26.9

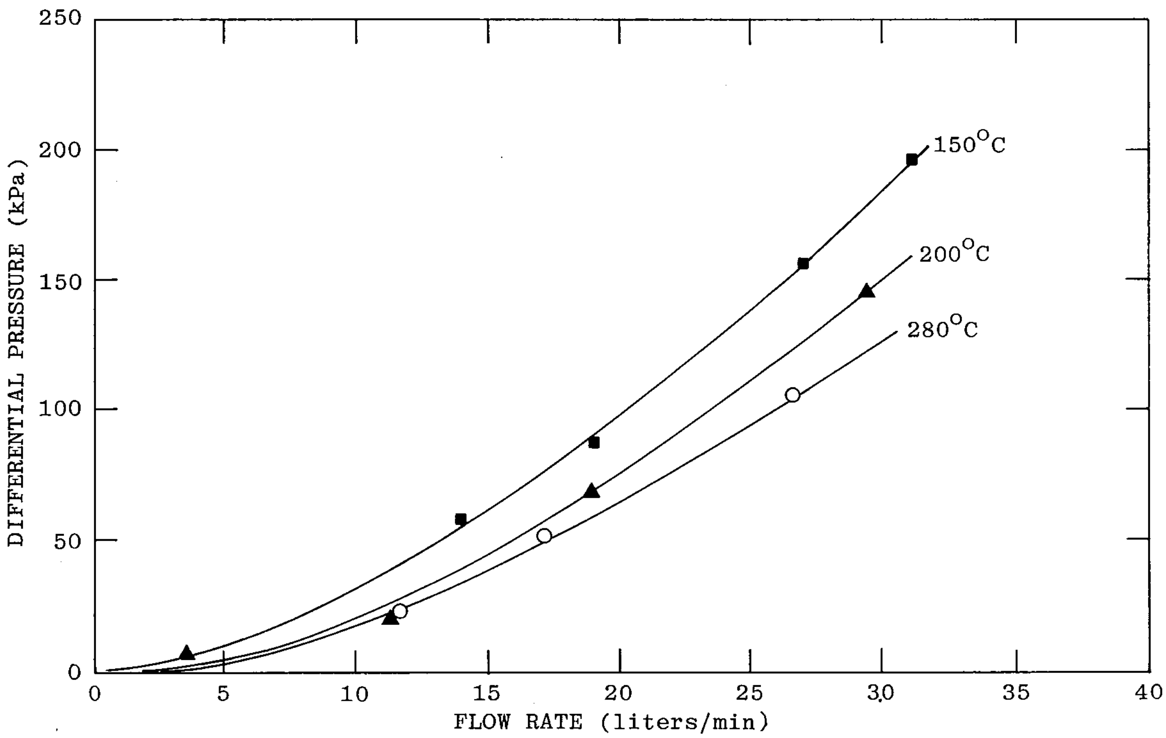

Figure 10. Hexcel Receiver Tube Differential Pressure.

Results from the absorber tube absorptance and emittance measurements are shown in Table 4. The data indicate less than the normal as plated absorptance of ≥0.95. Emittance was also less than the normally observed values of ε_{th} (300°C) ≤0.25.

Table 4. Absorptance/Emittance

Location	α		ε_{th} (100°C)		ε_{th} (300°C)	
	Before	After	Before	After	Before	After
Position 1	0.92	0.91	0.12	0.11	0.18	0.17
Position 2	0.92	0.93	0.12	0.15	0.17	0.18
Position 3	0.89	0.87	0.11	0.11	0.16	0.15
Position 4	0.79	0.72	0.21	0.17	0.22	0.21

The absorptance and emittance measurements made after conclusion of the thermal testing are also shown in Table 4. The measured values were nearly the same as the pre-test values (within the accuracy of the measurement) except near the outlet end of the receiver tube. These values had decreased, as shown in the last line of Table 4.

A partial time-temperature history of the absorber tube was obtained from the test data as a possible aid in determining reasons for the degradation of the black chrome surface. This data is shown in Table 5, revealing a total of about 33 hours at temperatures above 200^{o}C during testing at Sandia's CMTF. An unknown amount of testing at unknown temperatures had also been done by Hexcel prior to shipping the collector module to Sandia.

Table 5. Hexcel Absorber Tube
Time-Temperature History

Approximate Temperature (°C)	Time in Focus hr:min	Time out of Focus hr:min	Total Time hr:min
200-225	10:15	4:45	15:00
225-250	8:00	2:30	10:30
250-300	5:30	2:00	7:30

Total Absorber Tube Time Over 200^{o}C = 33 Hours

SUMMARY OF RESULTS AND CONCLUSIONS: The Hexcel collector was the most efficient yet tested in the Sandia Collector Module Test Facility. At 160^{o}C output fluid temperature, 64% of the sun's energy entering the collector aperture was recovered; this efficiency dropped to 56% at 300^{o}C outlet temperatures. As can be seen from the data plotted in Figure 7, no correlation was apparent between efficiency and flow-rates tested, indicating excellent heat transfer even at low flow-rates.

The thermal efficiency of this collector design could be improved in two areas: (1) the absorber tube's black chrome coating absorbed less of the incoming energy than would be expected for a good black chrome plating, and (2) the thermal losses from all sources were greater than several other collectors tested.

Hexcel has estimated (Reference 3) that an optimum black chrome absorber would have increased peak noon efficiency by about 4%. Reasons for the rapid degradation of the absorber tube's black chrome coating at operating temperatures is unknown at present. This phenomenon has been observed on a few other receiver tubes after short exposure times, but has not occurred on others after long exposure at operating temperatures. Investigation is underway by Sandia Laboratories and others.

When compared to other systems recently tested, the losses per meter of the absorber tube were about twice as large, indicating that an improved design might reduce losses and thereby further increase efficiency. The receiver design as tested was not well sealed at the ends and had several small gaps in the glass covers, allowing some air circulation to carry away heat. A counterbalancing advantage to this glass cover design is the ease with which a section of glass could be replaced if broken.

The insulation layer behind the absorber tube was thinner than seen in some other insulated designs; Hexcel has already changed their design to increase insulation and reduce losses from this area (Reference 3).

Another possible contributor to losses was the aluminum secondary reflector behind the absorber tube. A recent NASA study (Reference 5) reported that a reflector of ALZAK material similar to that used by Hexcel returned only about 55% of incident energy compared to an expected 80% reflectivity. Sandia measurements have been less pessimistic, reporting reflectivities in the 70-75% range (Reference 6).

The composite magnitude of improvements in all these areas is hard to estimate, but if a 40% loss reduction were achieved, to bring this collector's receiver losses near those of the lowest loss receiver tested at the CMTF, the result would be an increase of more than 4% in peak noon efficiency.

Because the heat losses are relatively constant, while total heat recovery in the fluid decreases steadily off-noon, such a reduction in losses is even more desirable when considering the increase in energy recovered throughout an 8-hour day. At 300^{o}C, 8.3% more heat would be recovered at noon, 18% at three hours from noon, and 44% more heat recovery at four hours from noon.

The internally finned, plugged absorber tube design was quite effective in producing turbulent fluid flow and efficient heat transfer; no improvement in efficiency was apparent as flow-rates were increased. However, the differential pressures measured were relatively high, indicating high pressure drops in a large collector field and the requirement for high pumping power. For comparison, results from tests on another collector's similarly sized absorber tubes are instructive. The other absorber tube was 2.5 cm in diameter vs 3.81 cm for Hexcel, 12.2 m in length vs. 6.4 m for Hexcel, and contained no plug or other turbulence producing device. This design did exhibit some sensitivity of efficiency to flow-rate (about 2-3%) but produced pressure drops more than an order of magnitude smaller at similar flow-rates and temperatures, even using a tube nearly twice as long.

Although some improvements are possible as indicated above, the Hexcel collector design is an excellent one. It was higher in efficiency than others tested, mechanically simple, relatively light in weight, and rugged enough to obtain a long lifetime in the field.

REFERENCES

1. Solar Total Energy Program Plan, SAND76-0167 (revised), August 1976, Sandia Laboratories, Albuquerque, New Mexico.

2. Harrison, T.; Dworzak, W.; and Folkner, C., Solar Collector Module Test Facility, Instrumentation Fluid Loop Number One, SAND76-0425, January 1977, Sandia Laboratories, Albuquerque, New Mexico.

3. Parker, D., Test Results of Hexcel Parabolic Trough Solar Concentrator at Sandia Collector Module Test Facility in Albuquerque, NM, Document 178-DAP-#1, January 1978, Hexcel Corp., Dublin, California.

4. Therminol 66, Technical Data Sheet, IC/FF-35, Monsanto Company.

5. Hastings, L,; Allums, S.; and Jensen W., An Analytical and Experimental Investigation of a 1.8 by 3.7 Meter Fresnel Lens Solar Concentrator, NASA Technical Paper 1005, August 1977, Marshal Space Flight Center, Alabama.

6. Pettit, R. B., Characterization of the Reflected Beam Profile of Solar Mirror Materials, SAND76-0537, 1976, Sandia Laboratories, Albuquerque, New Mexico.

DISTRIBUTION:
TID-4500-R66, UC-62 (316)

Aerospace Corporation
2350 E. El Segundo Blvd.
El Segundo, CA 90245
Attn: Leon Bush

American Gas Association
1515 Wilson Boulevard
Arlington, VA 22209
Attn: P. Susey

Barber Nichols Engineering
6325 W. 55th Avenue
Arvada, CO 80002
Attn: R. G. Olander

Battele Memorial Institute
Pacific Northwest Laboratory
P.O. Box 999
Richland, WA 99352
Attn: K. Drumheller

Brookhaven National Laboratory
Associated Universities, Inc.
Upton, LI, NY 11973
Attn: J. Blewett

Congressional Research Service
Library of Congress
Washington, DC 20540
Attn: H. Bullis

Del Manufacturing Co.
905 Monterey Pass Road
Monterey Park, CA 91754
Attn: M. M. Delgado

Department of Energy
Albuquerque Operations Office
Albuquerque, NM 87115
Attn: D. K. Nowlin
G. W. Rhodes
J. R. Roder

Department of Energy
Solar Technology Division
Washington, DC 20545
Attn: G. W. Braun
G. M. Kaplan
H. H. Marvin
J. E. Rannels

Department of Energy
Storage Division
Washington, DC 20545
Attn: C. J. Swet

Desert Research Institute
Energy Systems Laboratory
1500 Buchanan Blvd.
Boulder City, NV 89005
Attn: Jerry O. Bradley

Honorable Pete V. Domenici
Room 405
Russell Senate Office Bldg.
Washington, DC 20510

Edison Electric Institute
90 Park Avenue
New York, NY 10016
Attn: L. O. Elsaesser
Director of Research

Energy Institute
1700 Las Lomas
Albuquerque, NM 87131
Attn: T. T. Shishman

Gas Company
723 Silver, SW
Albuquerque, NM 87103
Attn: B. D. Daugherty

General Electric Company
Valley Forge Space Center
Valley Forge, PA 19087
Attn: Walt Pijawka
Ron Hodge

General Electric Company
P.O. Box 8661
Philadelphia, PA 19101
Attn: A. J. Poche

Georgia Power Company
Economic Services, VP
Atlanta, GA 30302
Attn: Mr. Walter Hensley

Grumman Corporation
4175 Veterans Memorial Highway
Ronkonkoma, NY 11779
Attn: Ed Diamond

Honeywell, Inc.
2600 Ridgeway Parkway
Minneapolis, MN 55413
Attn: B. P. Gopta,
MS MN17-T789

Jet Propulsion Laboratory
Bldg. 277, Rm 201
4800 Oak Grove Drive
Pasadena, CA 91103
Attn: V. C. Truscello

Lawrence Berkely Laboratory
University of California
Berkley, CA 94720
Attn: Dr. Mike Wallig

Lawrence Livermore Laboratory
University of California
P.O. Box 808
Livermore, Ca 94500
Attn: W. C. Dickinson

DISTRIBUTION (Cont.):

Honorable Manuel Lujan
1323 Longworth Building
Washington, DC 20515

R. L. San Martin
New Mexico State University
Las Cruces, NM 88001

Oak Ridge Operations Office, DOE
P.O. Box Y
Oak Ridge, TN 37830
Attn: J. R. Blevins
J. Johnson
S. I. Kaplan
R. Pearlstein

Office of Science and Technology
Executive Office of the President
Washington, DC 20506
Attn: R. Balzhizer

Office of Technology Assessment
Old Immigration Building, Rm 722
119 D. Street, NE
Washington, DC 20002

Honorable Harold Runnels
1535 Longworth Building
Washington, DC 20515

Honorable Harrison H. Schmitt
Room 1251
Dirksen Senate Office Bldg.
Washington, DC 20510

Solar Energy Research Institute
1536 Cole Blvd.
Golden, CO 80401
Attn: Charles Grosskreutz

Solar Kinetics, Inc.
P.O. Box 10764
Dallas, TX 75207
Attn: Gus Hutchison

Sundstrand Electric Power
4747 Harrison Avenue
Rockford, IL 61101
Attn: A. W. Adam

Suntec Systems, Inc.
21405 Hamburg Avenue
Lakeville, MN 55044

TEAM, Inc.
8136 Old Keene Mill Road
Springfield, VA 22152
Attn: J. H. Davision

Tennessee Energy Office
Suite 250, Capitol Hill Bldg.
Nashville, TN 37219
Attn: Carroll V. Kroeger, Sr.

University of Arkansas
Mechanical Engineering Department
Fayetteville, AR 72701
Attn: Dr. F. K. Deaver

University of Delaware
Institute of Energy Conversion
Newark, DE 19711
Attn: K. W. Boer

University of New Mexico
Department of Mechanical Engineering
Albuquerque, NM 87113
Attn: W. A Cross
M. W. Wilden

US Department of Interior
Room 5204
Washington, DC 20204
Attn: M. Prochnik

Watt Engineering Ltd.
RR1, Box 183 1/2
Cedaredge, CO 81413
Attn: A. D. Watt

1100 C. D. Broyles
1260 K. J. Touryan
1262 H. C. Hardee
1280 T. B. Lane
1284 R. T. Othmer
1300 D. B. Shuster
1330 R. C. Maydew
2300 J. C. King
2320 K. L. Gillespie
2323 C. M. Gabriel
2324 L. W. Schulz
2326 G. M. Heck
3161 J. E. Mitchell
3700 L. S. Conterno
5000 A. Narath
5200 E. H. Beckner
5231 J. H. Renken
5700 J. H. Scott
5710 G. E. Brandvold
5711 J. F. Banas
5712 J. A. Leonard
5713 B. W. Marshall
5714 R. P. Stromberg
5715 R. H. Braasch
5719 D. G. Schueler
5730 H. M. Stoller
5740 V. L. Dugan
5800 R. S. Claassen
Attn: R. G. Kepler, 5810
R. L. Schwoebel, 5820
5830 M. J. Davis
5831 N. J. Magnani
5834 D. M. Mattox
5840 H. J. Saxton
5842 J. N. Sweet
5844 F. P. Gerstle
5846 E. K. Beauchamp
8100 L. Gutierrez

DISTRIBUTION (Cont.):

8130 R. C. Wayne
8131 W. G. Wilson
8132 A. C. Skinrood
8313 R. W. Mar
9330 A. J. Clark, Jr.
9340 W. E. Caldes
9350 F. W. Neilson
9352 O. N. Burchett
9400 H. E. Lenander
9572 L. G. Rainhart
9700 R. E. Hopper
Attn: H. H. Pastorius, 9740
R. W. Hunnicutt, 9750
6011 G. C. Newlin
8266 E. A. Aas
3141 C. A. Pepmueller (5)
3151 W. L. Garner (3)
For DOE/TIC
(Unlimited Release)
DOE/TIC (25)
(R. P. Campbell, 3172-3)